Removal of dissolved oxygen using non-porous hollow-fiber membranes

Akira Ito[a,*], Kazuaki Yamagiwa[a], Masato Tamura[a], Michio Furusawa[b]

[a]*Departmemt of Chemical and Material Engineering, Niigata University, Ikarashi 2-8050, Niigata 950-21, Japan*
[b]*Nagayanagi Kougyou Co., Kyoujima 1-1-1, Tokyo 131, Japan*

Abstract

The removal of dissolved oxygen (DO) from water was studied using a silicone rubber hollow-fiber membrane module. Dissolved oxygen in water was effectively reduced by the vacuum degassing or pervaporation process through a non-porous membrane. The controlling transport property, gas permeability through the membrane, was independently measured by a method using a differential transformer. A gas-phase driving force model was presented based on the permeabilities of the permeates through the hollow-fiber. Experimental results of the oxygen removal from water were compared with the model calculations. The present model proved to explain the effects of the pressure condition and the operation mode on the removal of oxygen from water. Although the liquid-phase mass transfer resistance was shown to have a large effect on the removal performance of the membrane module, the membrane permeation step controlled the mass transfer during vacuum degassing. © 1998 Elsevier Science B.V.

Keywords: Fiber membranes; Gas and vapor permeation; Pervaporation; Water treatment; Dissolved oxygen

1. Introduction

The removal of dissolved oxygen (DO) from water is needed today in many production areas such as semiconductors, pharmaceuticals and foods. In the power industry, corrosion in a boiler or steel pipes will be prevented if the DO level in the water is lower than 0.5 ppm. There have been several methods available to remove DO from water, such as a thermal or vacuum degassing process, and the chemical reduction process using sodium bisulfite.

The membrane separation process has a possible candidate as a removal process for DO. Several vacuum degassing processes using a membrane are commercially available today, e.g., a process by Hoechest Celanese, USA. This kind of process uses hydrophobic and microporous membranes or hollow-fibers.

A vacuum is applied to one side of the microporous membrane, and DO in the feed water will be removed through it. The mass transfer process of DO through a microporous membrane has been well studied [1–3]. There have been related studies [4,5] concerning the design of an artificial gill.

---

*Corresponding author. Tel.: +81 25 262 6789; fax: +81 25 262 6789; e-mail: aito@eng.niigata-u.ac.jp

As another membrane process for degassing, a non-porous membrane is also applicable. Such a process using a non-porous membrane has several advantages. For example, the permeate side pressure will be arbitrarily chosen, since feed water would not penetrate to the other side of the membrane. There have been a few studies on the degassing process using a non-porous membrane. Baker et al. [6] reported the separation of oxygen from sea water using a composite membrane. Their objective was the use of oxygen dissolved in sea water for a submarine life-support system and for a fuel cell. They treated the permeation process as a kind of pervaporation, but provided little theoretical information about it.

Oxygen permeation through a non-porous membrane has been theoretically studied for the water/membrane/water system [7–10]. Hwang et al. [10] reported the oxygen transfer rates between two water streams through a silicone rubber flat sheet. They apparently evaluated the permeability of oxygen through the non-porous membrane from the view point of the gas-phase driving force. Their conclusion was that the apparent permeability agreed with the gas-phase permeability, which was measured during the gas-phase permeation [11]. In addition, they insisted that the liquid-phase mass transfer resistance will play a large part in the mass transfer of oxygen from water through the membrane.

The objective of this study is to develop a model based on the permeabilities of permeate gas and vapor for the removal process of DO using a silicone rubber hollow-fiber membrane module. The controlling transport property of the process, permeability through the membrane, was independently measured by a new method using a differential transformer. A model based on the gas and water vapor permeabilities for the simultaneous transport of oxygen, nitrogen and water through the non-porous membrane was presented and experimentally tested.

2. Permeability through silicone rubber microtube

The permeation model based on the gas-phase driving force will require the permeability of the permeates in the gas or vapor state. In this study, a membrane module made by silicone rubber microtubes was used for the DO removal process. The permeabilities of oxygen, nitrogen and water vapor through the silicone rubber microtube were independently measured. The microtube is a silicone rubber hollow-fiber with a 320 µm o.d. and 200 µm i.d., which was purchased from Nagayanagi Kougyou, Japan [12]. A small membrane module with a 66 cm^2 permeation area was made using the microtubes and was used for the permeability measurement.

The precise measurement apparatus of permeability is shown in Fig. 1. The apparatus consists of a glass
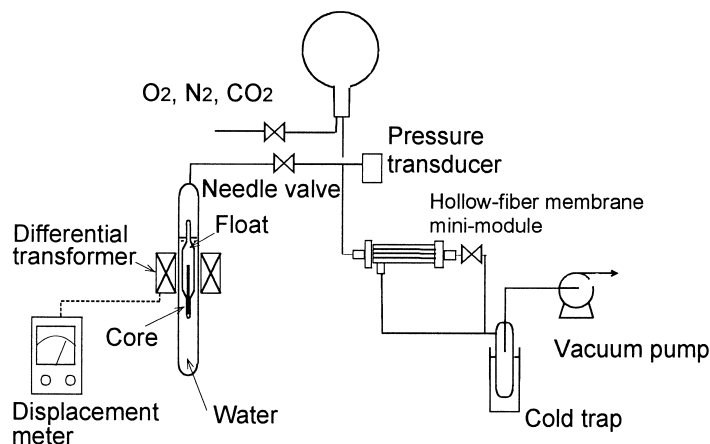

Fig. 1. Permeability measurement apparatus.

tube vessel for the liquid source, a gas reservoir, the mini-module for the hollow-fiber membrane, a cold trap and a vacuum pump. The permeate side pressure was maintained below 0.3 kPa in all runs. For a permeation run with water, the vapor was fed from the liquid source. The permeation rate of water vapor was measured based on the level change in the water vessel [13]. For a permeation run with a gas, the feed line of the membrane module was connected to the gas reservoir. The permeation rate of the gases through the membrane was measured based on the pressure change in the feed side line of known volume.

Fig. 2 shows the vapor permeabilities of water vapor, oxygen and nitrogen gas through the hollow-fiber membrane. The permeability of water vapor has been precisely measured at a low vapor pressure. The water vapor permeability significantly depends on the feed vapor pressure, and the permeability in the shell direction permeation is greater than that in the tube direction. These are the characteristics of vapor permeability through rubbery polymers [12]. On the other hand, the permeabilities of the gases, oxygen and nitrogen, have no dependency on the feed pressure and the permeation direction. These permeabilities well agree with that through a silicone rubber flat sheet membrane for water vapor [14] and for gases [11].
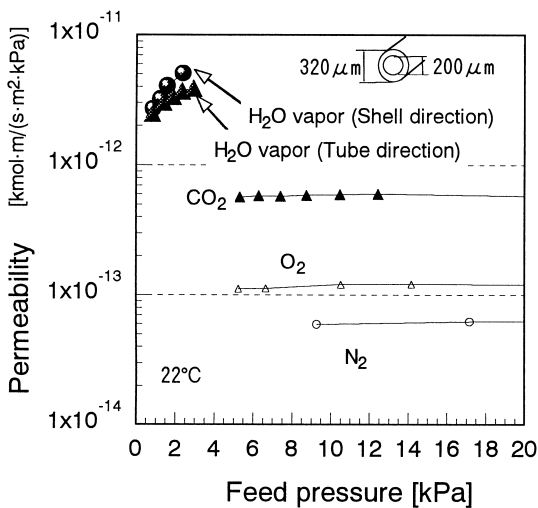

Fig. 2. Permeabilities of water vapor, oxygen and nitrogen through the hollow-fiber membrane.

3. Gas-phase driving force model for permeation of dissolved oxygen through a non-porous membrane

According to Hwang's results [10], oxygen transfer in a water/silicone rubber membrane/water system is about the same as in the case of gas-phase permeation. That is, the oxygen flux in the water/non-porous membrane/water system will be described by the permeability and gas-phase equilibrium partial pressures, except for the effect of liquid film resistance.

Although permeate side conditions are different from that system, the gas-phase driving force model is applied to a vacuum degassing process with a non-porous membrane. In the vacuum degassing process, permeate side pressure will be practically at a partial vacuum higher than the saturation water vapor pressure at the operating temperature. Therefore, the oxygen transfer rate will be affected by the permeate side partial pressures of other permeate gases or vapors. A model calculation for the vacuum degassing process will need to be treated as a simultaneous transfer of dissolved gases and water vapor.

In our experimental setup, feed water flows through the tube side of the membrane module, and permeate flows co-currently through shell side. The changes in the molar flow rates of each component along the flow direction in the membrane module, F_i and V_i, are described by the permeabilities, Q_i, and the vapor phase driving forces:

$$-dF_{O_2}/dA = dV_{O_2}/dA = Q_{O_2}(p^*_{O_2} - P_l y_{O_2})/\delta \quad (1)$$

$$-dF_{N_2}/dA = dV_{N_2}/dA = Q_{N_2}(p^*_{N_2} - P_l y_{N_2})/\delta \quad (2)$$

$$-dF_{H_2O}/dA = dV_{H_2O}/dA = Q_{H_2O}(p^*_{H_2O} - P_l y_{H_2O})/\delta \quad (3)$$

where F is the molar flow rate in the feed and V is that in the permeate mixed gas. The permeabilities of each component have been independently measured, which is shown in Fig. 2. Applying a plug-flow model, the permeate side concentrations are the fraction of molar flow rates in the shell side of the membrane module:

$$y_i = V_i / \Sigma V_i \quad (i = O_2, N_2, H_2O) \quad (4)$$

Equilibrium partial pressures of the dissolved gases are calculated using Henry constants:

$$p^*_i = H_i x_{si} \quad (i = O_2, N_2) \quad (5)$$

In a more precise model including the effect of the liquid side mass transfer resistance, the Hausen equation [15] for the mass transfer of laminar flow in a tube will give the concentration difference of the dissolved gas between the bulk flow and the membrane interface:

$$Sh = 3.66 + \frac{0.0668(D/l)Re\,Sc}{1 + 0.04[(D/l)Re\,Sc]^{2/3}} \qquad (6)$$

$$x_i - x_{si} = -\frac{(\mathrm{d}F_i/\mathrm{d}A)D}{Sh \cdot cD_{ABi}} \quad (i = \mathrm{O_2, N_2}) \qquad (7)$$

Under the assumption of plug-flow conditions on both sides of the membrane module, simultaneous integration of these differential equations gives the flow rate changes and concentration profiles of each component along the module [16]. The model calculation provides the DO concentration of the outlet flow of the membrane module. Considering all permeates including nitrogen, the present model could be applied to other related membrane processes, such as oxygen removal by a nitrogen purge or an oxygen supply from air to water.

4. Experimental

Fig. 3 shows the apparatus for the removal of DO from water.

A silicone rubber microtube membrane module (effective length: 14 cm; number of tubes: 6000; effective membrane area: 4950 cm^2) was made by Nagayanagi, Japan, with the same microtubes used in the permeability measurement. Ultra pure water with an adj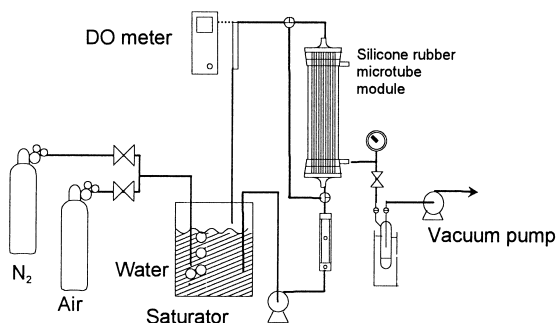usted oxygen concentration was fed into the tube side of the membrane module. The shell side of the module was evacuated by a vacuum pump. The permeate side pressure was controlled by a vacuum regulator (Kendall Model 16, Fairchild). The DO concentrations of the inlet and outlet flows were measured by a DO meter (Horiba OM12). The operation parameters in the experiments were the permeate side pressure and the feed flow rate.

5. Results and discussion

Fig. 4 shows the effect of the permeate side pressure on the DO removal efficiency of the vacuum degassing process. The feed flow rate was kept constant and the permeate side pressure was changed. As the permeate side pressure decreased, the DO level of the outlet flow approached a minimum value. DO could be effectively removed by the vacuum degassing process using a non-porous membrane.

The model calculations have been compared with the experimental results under the same operating conditions. The solid curve in the figure is the calculation results including the liquid-phase mass transfer resistance. The present model provides a good prediction of effect of the permeate side pressure over the range from vacuum to partial vacuum. The model will

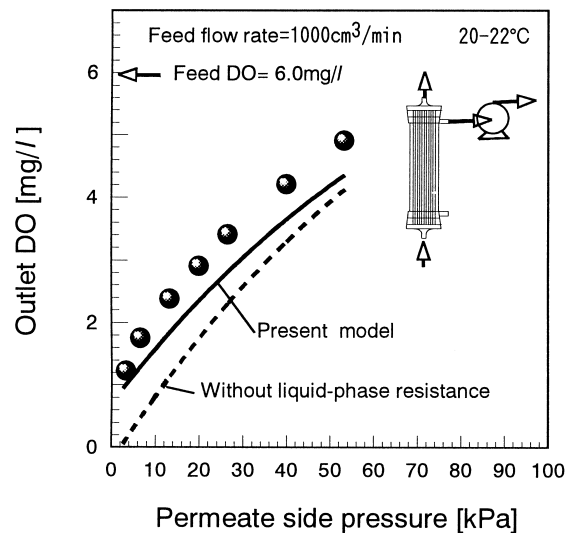Fig. 3. Experimental apparatus for removal of DO.

Fig. 4. The effect of permeate side pressure to the DO removal efficiency of the vacuum degassing process.

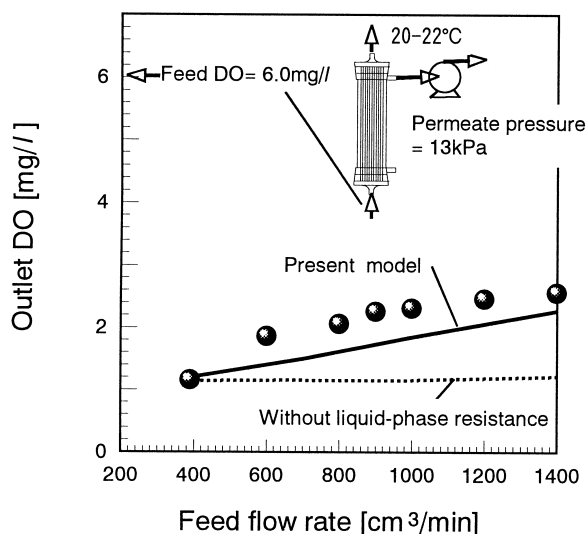Fig. 5. The effect of feed flow rate on the DO removal efficiency.

Fig. 6. DO removal process using a sweep gas (nitrogen).

do the calculating using various permeate side pressure, because of considering all permeation fluxes including nitrogen and water vapor. The difference between experimental data and the solid line is explained by a deviation from plug-flow model for the permeate side flow. An increasing of permeate side pressure will cause an uniform flow through the hollow-fiber bundle. The dashed line in the figure represents another calculation result for a case without liquid-phase resistance, where the mass transfer resistance in water was neglected ($x_i = x_{si}$). During the vacuum degassing process, the liquid-phase mass transfer resistance is part of the total resistance.

Fig. 5 shows the effect of feed flow rate on the DO removal efficiency of the membrane module. The permeate side pressure was kept at a moderate vacuum of 13 kPa and the feed flow rate was changed in the range of laminar flow. The DO of 6 mg/l in the feed water was reduced to 2 mg/l in the outlet flow. When the feed flow rate decreases, the OD of the outlet flow decreases.

In the figure, the dashed line represents the calculated result of a case without liquid-phase resistance. In this case, the model will predict a small effect of flow rate on the outlet DO. This is because that the membrane module was long enough for the feed flow to approach an equilibrium concentration with the permeate side. So, if the liquid-phase resistance is
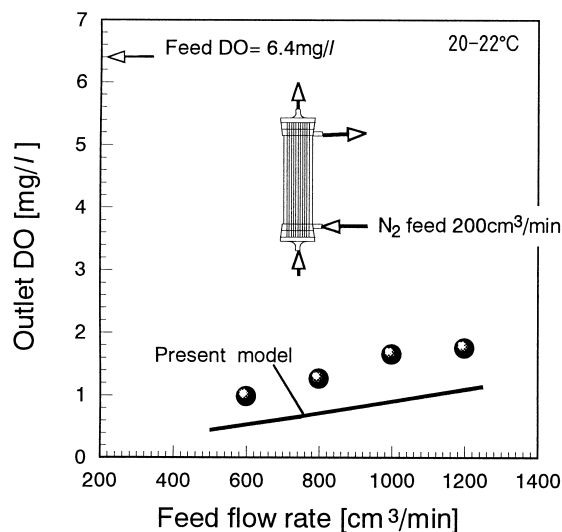
ignored, the outlet DO will be only slightly affected by the flow rate. The solid line is the model calculation including the liquid-phase mass transfer resistance. The prediction by the model is improved by considering the liquid-phase mass transfer. The difference between experimental data and the solid line is explained by the effect of ununiformity in permeate side flow. Although the liquid-phase resistance is more important with an increase in the feed flow rate, the membrane permeation step is shown to control the entire mass transfer process of vacuum degassing.

Since the model is a simple and general description of permeation through a non-swelling membrane, we can apply it to other applications. Another DO removal process uses a nitrogen flow in the permeate side as a sweep gas. Fig. 6 shows the results of this type of experiments. Feed DO is effectively reduced during this mode of operation. A model calculation was done using the same equations as the vacuum degassing, where the partial pressure of nitrogen was set to atmospheric pressure at the inlet of the module. Present model also predicts entire tendency of DO removal process. A failure of the model would be attributed to the non-ideal flow of the shell side flow.

Fig. 7 shows the results of another operation involving oxygen feed from air to water. The low DO water was fed to the membrane module and air flowed co-currently through the shell side. Oxygen in the air on
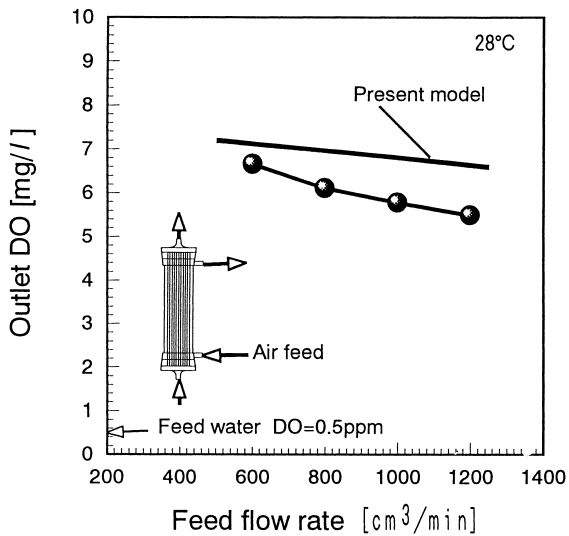
Fig. 7. Oxygen transfer from air to water through the membrane.

the shell side of the module dissolves in the water through the membrane. During this type of process, the direction of oxygen transfer is the reverse of the DO removal process. This mode of mass transfer is referred to as an artificial gill. The DO of the feed water increases from 0.5 ppm at the inlet to nearly the saturation DO level of air. The feed flow rate affects the DO feed efficiency of the module. In the figure, the solid line is the calculation result of the present model. In the calculation, model equations and transport properties were the same as that for the DO reduction process. Only the driving force of the oxygen is negative compared to the DO removal process. The present model also predicts the entire tendency of DO supply process. A failure of the model would be attributed to the non-ideal flow of the shell side feed gas.

6. Conclusions

A model consideration for the removal of dissolved oxygen (DO) from water using a silicone rubber hollow-fiber membrane module was presented and compared for the experimental results. The model was able to explain the effects of pressure conditions and operation mode on the removal of oxygen from water. The present model would be applicable to other

processes of oxygen transfer into or from water through a non-porous membrane.

The present gas-phase driving model with liquid-phase resistance has been proven to be the basis for the oxygen transfer process through a non-porous membrane to water. Originally, the gas-phase driving force model has been applied to a pervaporation process [14]. One could treat pervaporation, vacuum degassing and an artificial gill with a non-porous membrane from the same view point of permeability. For a more precise prediction, we must consider the effect of gas-phase mixing on the shell side flow of the hollow-fiber membrane module.

7. List of symbols

A	permeation area of the membrane module (m^2)
c	mole density of the feed (mol/m^3)
D	inner diameter of the hollow-fiber membrane (m)
D_{AB}	diffusion coefficient in water (m^2/s)
F_i	mole flow rate of a component in feed liquid (tube side) (kmol/s)
H	Henry constant (kPa)
l	distance from the inlet along flow direction (m)
P_l	permeate side pressure (kPa)
p^*	equilibrium partial pressure (kPa)
Q_i	permeability (kmol m/(s m^2 kPa))
Re	Reynolds number
Sc	Schmidt number
Sh	Sherwood number
V_i	mole flow rate of a component in permeate gas flow (shell side) (kmol/s)
x_i	DO or nitrogen concentration in bulk water flow (mole fraction)
x_s	DO or nitrogen concentration in water on the membrane surface (mole fraction)
y_i	mole fraction of ith component in permeate flow
δ	membrane thickness (m)

References

[1] M.S.L. Tai, I. Chau, K. Li, W.J. Ng, W.K. Teo, Removal of dissolved oxygen in ultrapure water production using

microporous membrane modules, J. Membr. Sci. 87 (1994) 99–105.

[2] Y. Kasama, Y. Yagi, T. Imaoka, M. Kawakami, T. Ohmi, Advanced D.I. Water system with low dissolved oxygen for ULSI processing, Proceedings, Institute of Environmental Sciences, 1990, pp. 344–349.

[3] T. Leiknes, M.J. Semmens, C. Gantzer, The performance of a membrane vacuum degasser, Effective Membrane Processes – New Perspectives, Mechanical Engineering, London, 1993, p. 341.

[4] L.W. Lund, W.J. Federspiel, B.G. Hattler, Gas permeability of hollow fiber membranes in a gas–liquid system, J. Membr. Sci. 117 (1996) 207–219.

[5] J. Kamo, M. Uchida, T. Hirai, H. Yoshida, K. Kamada, T. Takemura, A new multilayered composite hollow fiber membrane for artificial lung, Artificial Organs 14 (1990) 369–372.

[6] C.M. Bell, P. Chow, R.W. Baker, Separation of oxygen from seawater by membrane permeation, AD Report, AD-A-208 863 (1989).

[7] H. Yasuda, W. Stone, Permeability of polymer membranes to dissolved oxygen, J. Polym. Sci., A-1 4 (1966) 1314–1316.

[8] H. Yasuda, Basic consideration of permeability of polymer membrane to dissolved oxygen, J. Polym. Sci., A-1 5 (1967) 2952–2956.

[9] H. Yasuda, C.E. Lamaze, Transfer of gas to dissolved oxygen in water via porous and nonporous polymer membrane, J. Appl. Polym. Sci. 16 (1972) 595–601.

[10] S.-T. Hwang, T.E.S. Tang, K. Kammermeyer, Transport of dissolved oxygen through silicone rubber membrane, J. Macromol. Sci.-Phys. B 5(1) (1971) 1–10.

[11] R.M. Barrer, H.T. Chio, Solution and diffusion of gases and vapors in silicone rubber membranes, J. Polym. Sci. C 10 (1965) 111–138.

[12] A. Ito, K. Shirasuna, T. Iizzuka, M. Fujii, Recovery of organic vapors from nitrogen gas mixtures by use of silicone rubber hollow-fiber membranes, Kagaku Kogaku Ronbunshu 16 (1990) 295–301.

[13] Y. Feng, S. Honnma, A. Ito, Improved measurement device for vapor permeation and pervaporation, J. Appl. Polym. Sci. 63 (1997) 433–438.

[14] A. Ito, K. Watanabe, Y. Feng, Swollen-dry-layer model for the pervaporation of ethanol–water solution through hydrophilic membranes, Sep. Sci. Tech. 30 (1995) 3045–3060.

[15] A.L. Hines, R.N. Maddox, Mass Transfer, Prentice-Hall, Englewood Cliffs, NJ, 1985.

[16] A. Ito, T. Iizuka, M. Fujii, O. Tozawa, Removal of dissolved chlorinated hydrocarbon solvents in water by pervaporation, Kagaku Kogaku Ronbunshu 16 (1990) 1269–1273.